

Study of Half-Metallic Ferromagnetism in $\text{Be}_{0.75}\text{Ti}_{0.25}\text{Y}$ ($\text{Y} = \text{S}, \text{Se}, \text{and Te}$) Using Ab Initio Calculations: Potential Candidate for Spintronic Devices

Q. Mahmood¹ · S. M. Alay-e-Abbas^{2,3} · Asif Mahmood⁴ · M. Yaseen⁶ · I. Mahmood⁵ · N. A. Noor⁵

Received: 6 October 2015 / Accepted: 7 December 2015 / Published online: 21 December 2015
© Springer Science+Business Media New York 2015

Abstract The structural, elastic, electronic, and magnetic properties of $\text{Be}_{0.75}\text{Ti}_{0.25}\text{Y}$ ($\text{Y} = \text{S}, \text{Se}, \text{and Te}$) have been investigated to understand their potential applications in spintronic devices. Crystals of BeS, BeSe, and BeTe, individually doped with Ti with a dopant concentration of $x = 0.25$, have been evaluated by using full-potential linearized augmented plane-wave plus local orbital method within the framework of density functional theory. We employed the Wu–Cohen generalized gradient approximation for optimizing the crystal structure and evaluating elastic properties. In order to improve bandgap values and optical parameters, the modified Becke and Johnson (mBJ) potential has been employed. The theoretical investigation of band structure

and density of states confirms the half-metallic ferromagnetic nature of these compounds. The elastic constants are calculated by the charpin method which shows that the compounds under consideration are brittle and anisotropic. Moreover, it is noted that tetrahedral crystal field splits the $3d$ state of Ti into triple degenerate t_{2g} and double degenerate e_g states. The exchange splitting energies $\Delta_x(d)$ and $\Delta_x(pd)$ and exchange constants ($N_0\alpha$) and ($N_0\beta$) are predicted from triple degenerate t_{2g} states, and negative values of $N_0\beta$ justify that the nature of effective potential is more attractive in spin down case rather than that in the spin up case. We also find the crystal field splitting ($\Delta E_{\text{crystal}} = E_{t_{2g}} - E_{e_g}$) energy and reduction of the local magnetic moment of Ti from its free space charge value and creation of small local magnetic moments on the non-magnetic Be, S, Se, and Te sites by p – d hybridization.

✉ N. A. Noor
naveedcsp@gmail.com

- ¹ Department of Physics, University of the Punjab, Quaid-e-Azam Campus, 54590 Lahore, Pakistan
- ² Department of Physics, Government College University Faisalabad, Allama Iqbal Road, 38000, Faisalabad, Pakistan
- ³ Department of Physics, University of Sargodha, 40100, Sargodha, Pakistan
- ⁴ College of Engineering, Chemical Engineering Department, King Saud University, Riyadh, Saudi Arabia
- ⁵ Department of Physics, University of Agriculture, Faisalabad 38040, Pakistan
- ⁶ Centre for High Energy Physics, University of the Punjab, Quaid-e-Azam Campus, 54590 Lahore, Pakistan

Keywords Ab initio calculations · Elastic parameters · Half-metallic FM semiconductor · Magnetic properties

1 Introduction

Doped semiconductors, usually known as disordered alloys of the type $\text{A}_{1-x}\text{B}_x\text{Y}$, can be experimentally achieved in AY semiconductors (e.g., ZnY, CdY, BeY, and MgY where $\text{Y} = \text{S}, \text{Se}, \text{Te}$) by replacing the cation A by the B counterpart [1–3]. Among these materials, the transition metal (TM)-doped AY semiconductors have attracted immense amount of attention from various research groups due to their potential usage in magnetic applications like magnetic recording and magnetic switching [4, 5]. In $\text{A}_{1-x}\text{B}_x\text{Y}$ materials, ferromagnetic (FM), antiferromagnetic (AFM), or spin-glass

(SG) behaviors can be achieved which depend upon the values of exchange interactions (i.e., d-d and the sp-d exchange) which exist between the dopant atom and the host species [4, 6]. The magnitude of these interactions can be ascribed to the hybridization between delocalized electrons in valence orbitals of the paramagnetic anion (usually the p states of chalcogenides) and the localized d states of the dopant atom [7, 8]. Several semiconductor compounds have

been proposed to achieve FM behavior at room temperature (RT) when doped with TM atoms. Some interesting examples of these materials include Cr-doped BeY [9] and CdTe [10], V-doped MgSe/Te [11], TM-doped GaN [12], and TM-doped ZnY [13, 14]. In this context, the BeY compounds have recently been subjected to investigations exploring the possibility of half-metallic ferromagnetic (HMF) behavior upon incorporation of TM dopant [9, 15]. The increasing interest in these materials stems from their higher covalent bonding, binding energies, and good mechanical properties [9]. Although the nature (intrinsic or extrinsic) of FM observed in TM-doped semiconductors is a topic of continued debate [16, 17], efforts are still required for providing useful information at the atomic level for understanding the physical properties of non-pristine semiconductors [18–20]. It is worth mentioning here that the concentration of B cation doped into the AY semiconductor has a large span and the achievement of particular opto-electronic response is fully dependent on its value.

The rapid development in the field of spintronics [21] has provided a strong stimulus to the realization of new magnetic materials. Among these materials, HMFs have accumulated huge attention due to their potential for use in spintronic devices. The investigation of these materials has enabled the understanding of spin-dependent devices such as giant magnetoresistance (GMR), tunneling magnetoresistance (TMR), junctions, and spin injectors. In HMF materials, the majority spins are liable for metallic properties and the minority spin density of states shows bandgap at the Fermi energy. Such activity extends in several perovskite structures [22], in Heusler compounds [23, 24], and in dilute magnetic semiconductors (DMSs) [25–27]. Apart from the magnetic ion-doped BeY investigations mentioned above [9, 14], no work has been reported on the properties of Ti-doped BeY compounds. In the present work, we aim to explore the ferromagnetism of Ti-doped BeY compounds and attain appropriate information of their properties by using ab initio spin-polarized density functional theory (DFT) calculations.

2 Method of Calculations

To determine the structural, elastic, electronic, and magnetic properties of $\text{Be}_{0.75}\text{Ti}_{0.25}\text{Y}$ ($\text{Y} = \text{S}, \text{Se}, \text{Te}$), the full-potential linearized augmented plane-wave plus local orbital (FP-LAPW + lo) method was applied using the simulation package WIEN2K [28]. In this method, eigenvalues and eigenfunctions are calculated for both spin up and spin down densities by solving two sets of Kohn–Sham equations (for single electron) self-consistently [29]. For the prediction of structural geometry, generalized gradient approximation (GGA) functional proposed by Wu

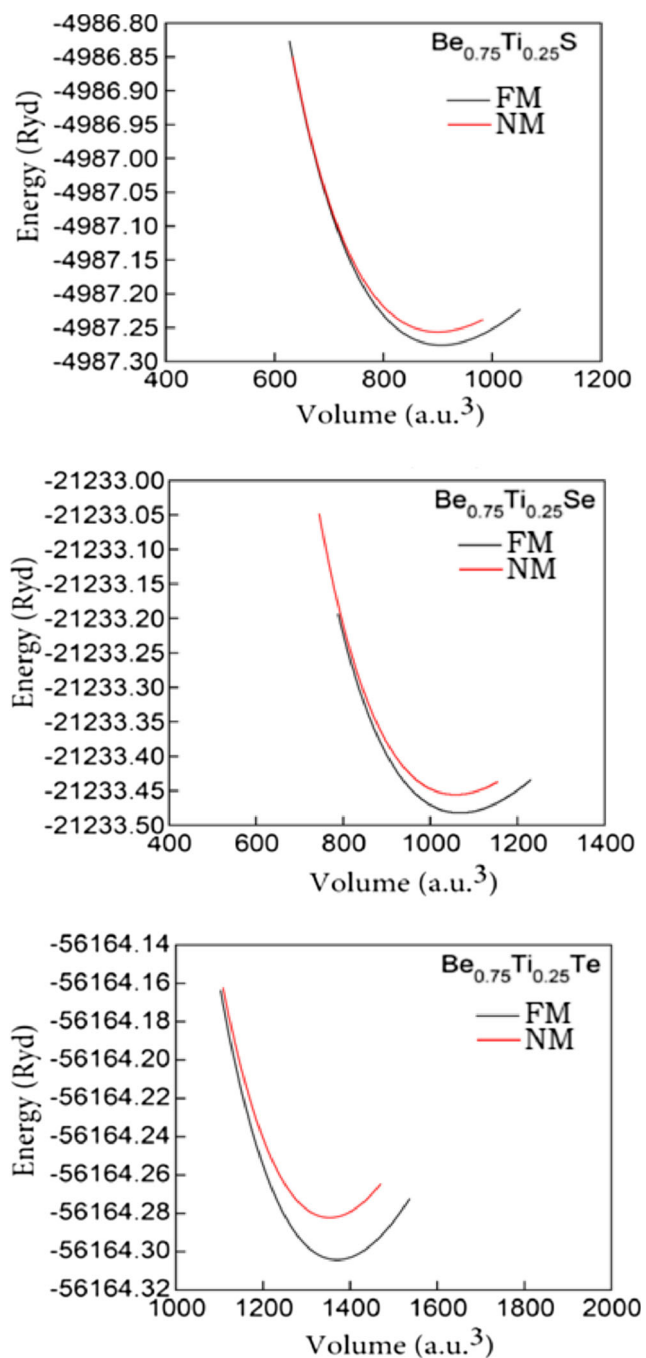


Fig. 1 Total energy versus unit cell volume for $\text{Be}_{0.75}\text{Ti}_{0.25}\text{Y}$ ($\text{Y} = \text{S}, \text{Se}, \text{Te}$) alloys in nonmagnetic (NM) and ferromagnetic (FM) phase

Table 1 Calculated lattice constants a_0 (Å), bulk modulus B_0 (GPa), bandgap E_g (eV), half-metallic gap E_{hm} (eV), total energy difference ΔE (eV), and enthalpy of formation H_f (eV) for the FM $Be_{1-x}Ti_xY$ ($Y = S, Se, Te$) at $x = 0, 0.25$

Compound	a_0 (Å)	B_0 (GPa)	E_g (eV)	E_{hm} (eV)	ΔE (eV)	ΔH (eV)
BeS (cal.)	4.85	99.26	4.07			
Others			3.13 ^d			
Exp.	4.87 ^a	105 ^a	5.50 ^c			–
Be _{0.75} Ti _{0.25} S	5.12	85.12	3.45	0.99	0.2653	0.6333
BeSe (cal.)	5.14	81.00	3.46			
Others			2.63 ^d			
Exp.	5.137 ^b	92.20 ^b	4.50 ^c			–
Be _{0.75} Ti _{0.25} Se	5.41	67.88	2.63	1.19	0.3607	0.6103
BeTe (cal.)	5.61	66.84	2.60			
Others			1.98 ^d			
Exp.	5.617 ^b	66.80 ^b	2.70 ^c			–
Be _{0.75} Ti _{0.25} Te	5.84	61.03	1.66	1.21	0.2998	0.5394

^aRef. [44], ^bRef. [45], ^cRef. [46], ^dRef. [47]

and Cohen [30] was employed to calculate exchange-correlation potential. Moreover, electronic and magnetic properties were determined by the combined implementation of local density approximation (LDA) correlation and modified Becke–Johnson exchange potential (mBJLDA). The modified Becke–Johnson exchange potential is based on semi-local exchange potential that gives a high degree of accuracy to calculate the band gap of wide band gap materials and transition metal-based materials [30–33]. In

FP-LAPW + lo method, the total volume of the charge density region is divided into non-overlapping muffin-tin region and inertial region, where the wave function of an electron is represented by spherical harmonics and plane waves, respectively.

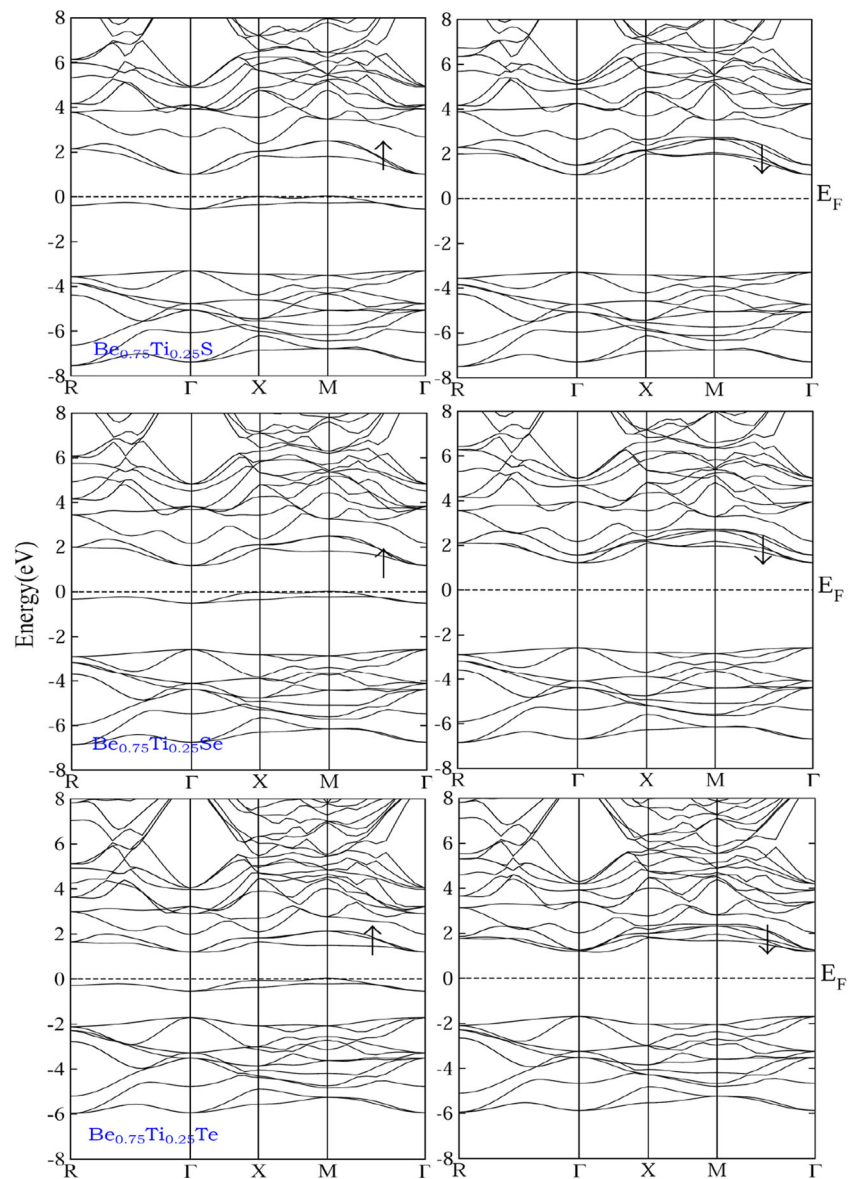
In zinc blende phase, the binary compound BeY ($Y = S, Se, \text{ and } Te$) has space groups F-43m (no. 216). The unit cell of this phase consists of Zn and Te atoms that are positioned at (0, 0, 0) and (1/4, 1/4, 1/4), respectively. In order

Table 2 Calculated elastic constants C_{ij} (GPa), Kleinman parameters (ζ), shear modulus G (GPa), Young’s modulus E (GPa), Poisson’s ratio, anisotropy factor, and B/G ratio at equilibrium for the parent compound and their alloys $Be_{1-x}Ti_xY$ ($Y = S, Se, \text{ and } Te$) at $x = 0, 0.25$

Compound	C_{11}	C_{12}	C_{44}	ζ	G	E	ν	A	B/G
BeS									
Cal.	172.2	74.67	106.2	0.568	77.71	187.6	0.208	2.16	1.37
Other cal.	184 ^a	75 ^a	99 ^a	–	73 ^a	174 ^a	0.19 ^a	–	–
Be _{0.75} Ti _{0.25} S									
This study (FM)	112.9	64.45	65.74	0.684	58.20	140.7	0.246	2.72	1.38
BeS									
Cal.	160.3	50.57	64.54	0.590	71.03	166.0	0.165	1.95	1.59
Other cal.	149 ^a	59 ^a	81 ^a		60 ^a	143 ^a	0.19 ^a		
Be _{0.75} Ti _{0.25} Se									
This study (FM)	93.73	56.39	56.77	0.714	36.39	92.82	0.255	3.04	1.69
BeTe									
Cal.	104.6	41.59	67.12	0.536	49.55	117.6	0.187	2.12	1.26
Other cal.	103 ^b	41 ^b	61 ^b		46 ^b	112 ^b	0.20 ^b		
Be _{0.75} Ti _{0.25} Te									
This study (FM)	86.29	39.41	50.62	0.588	37.16	90.99	0.243	2.16	1.48

^aRef. [48], ^bRef. [49]

Fig. 2 Spin-polarized band structures of $\text{Be}_{0.75}\text{Ti}_{0.25}\text{Y}$ ($\text{Y} = \text{S}, \text{Se}, \text{Te}$) alloys in majority spin (upwards arrow) and minority spin (downwards arrow) states using mBJLDA functional



to generate Ti-doped BeY compounds, we first constructed an eight-atom $1 \times 1 \times 1$ supercell of BeY compounds containing equal number of Be and Y atoms. The supercell was then used for constructing the doped structure by replacing one of the four Be atoms by the Ti dopant. The substitution of Ti into BeY ($\text{Y} = \text{S}, \text{Se}, \text{and Te}$) leaves the unit cell cubic with space group P-43m (no. 215). For the wave expansion inside the atomic sphere, the maximum quantum number l_{max} is taken as 10 and the Fourier-expanded charge density G_{max} up to $16 (\text{Ry})^{1/2}$. A k-mesh of $10 \times 10 \times 10$ has been taken in the irreducible part of the first Brillouin zone. The product of reciprocal lattice vector K_{max} and muffin-tin atomic radius R_{MT} controls the number of plane waves as $R_{\text{MT}} \times K_{\text{max}} = 8$. In this work, the muffin-tin radii of Be, Ti, S, Se, and Te are set to 1.98, 2.24,

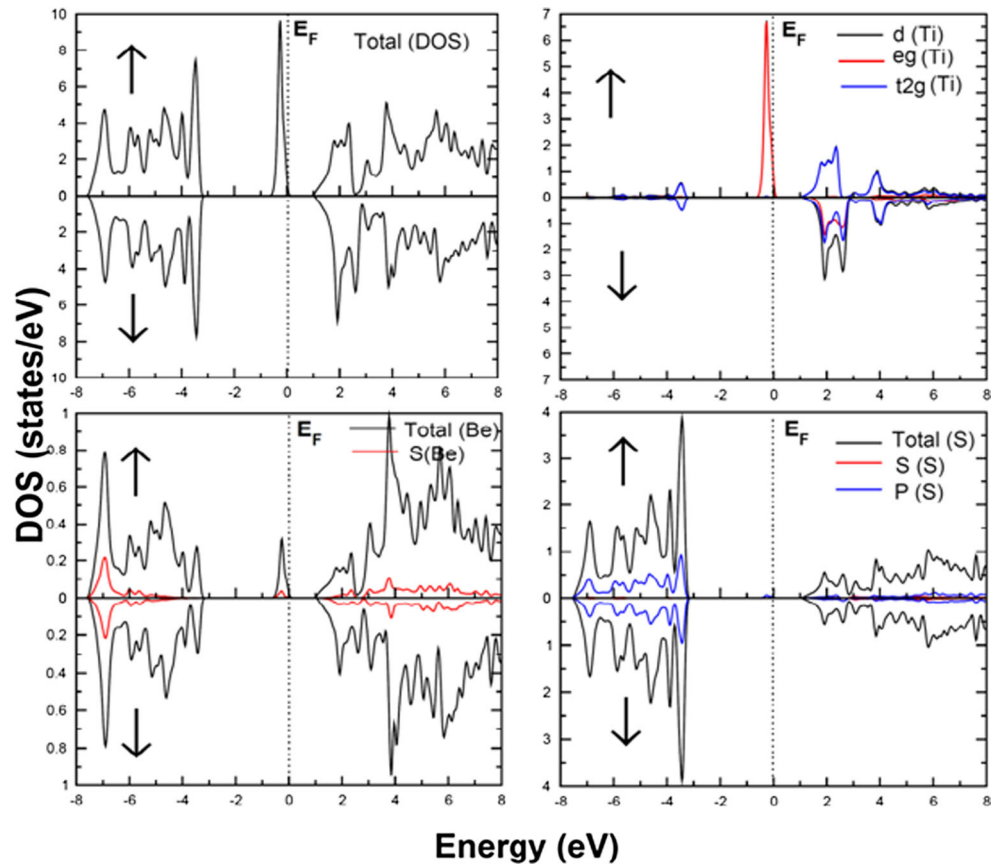
1.93, 2.00, and 2.04 a.u., respectively. For convergence of self-consistent calculations, we converge the total energy of crystal to a value less than 10^{-5} Ry by repetitive iterations.

3 Results and Discussion

3.1 Structural Properties

To investigate the ground-state lattice parameters of $\text{Be}_{0.75}\text{Ti}_{0.25}\text{Y}$ ($\text{Y} = \text{S}, \text{Se}, \text{and Te}$), we first calculate the total energy of each compound in paramagnetic and ferromagnetic phase using WC-GGA. The positive values of energy difference $\Delta E (\Delta E = E_{\text{NM}} - E_{\text{FM}})$ for Ti-doped BeY ($\text{Y} = \text{S}, \text{Se}, \text{and Te}$) confirm that at room temperature,

Fig. 3 Total density of states (TDOS) and partial density of states (PDOS) for $\text{Be}_{0.75}\text{Ti}_{0.25}\text{S}$ alloy for majority spin (upwards arrow) and minority spin (downwards arrow) configuration using mBJLDA functional



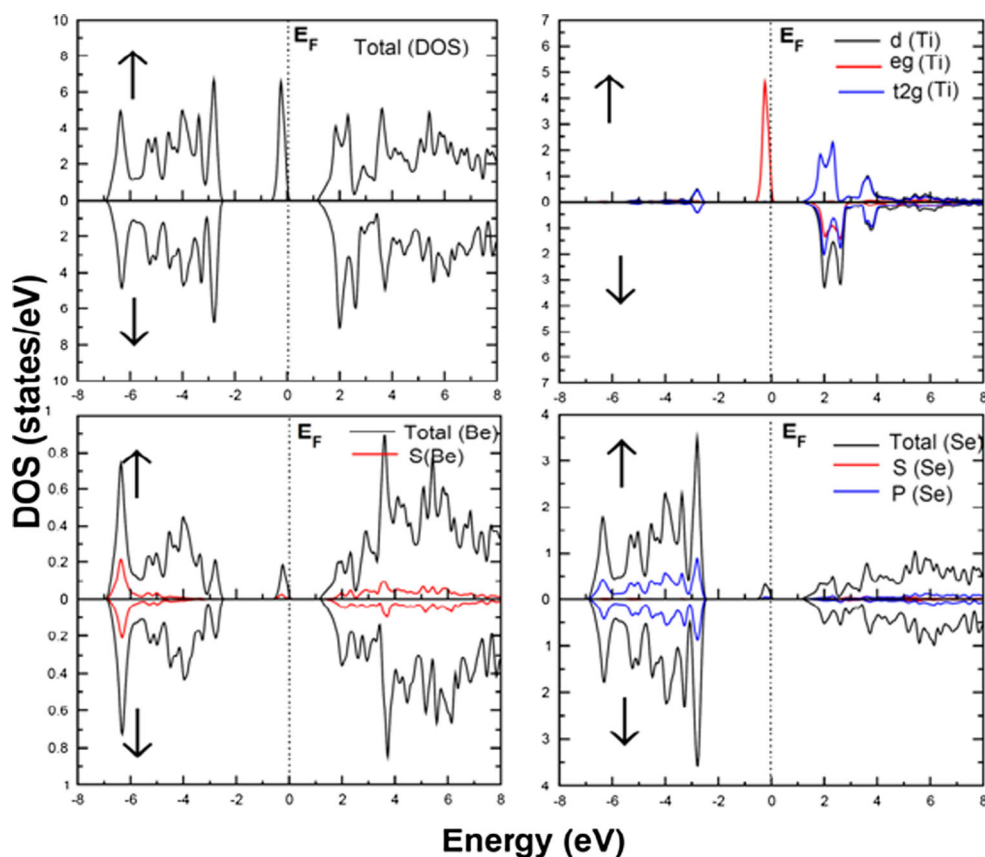
the ferromagnetic state is more stable than the paramagnetic state (Fig. 1). The numerical values of calculated ΔE are also presented in Table 1. By using Murnaghan's equation of state [34], the calculated values of lattice parameters and bulk moduli for relaxed structures are shown in Table 1. Referring to Table 1, we find that the value of lattice parameter increases due to incorporation of Ti dopant, while the bulk modulus decreases compared to the binary BeY compounds.

It also worth mentioning here that the elastic stiffness of Ti-doped BeY compounds decreases compared to their binary counterparts since it is directly proportional to bulk modulus and inversely proportional to lattice parameter [35, 36]. Further, the large inter-atomic distance reduces the electrostatic interaction that, consequently, reduces the band gap (as discussed later). Moreover, the amount of ionicity of the bonding depends upon the electronegativity difference between cation and anion and has a direct relation with band gap. To confirm the stability of Ti-doped BeY (Y = S, Se, and Te) in ferromagnetic state, enthalpy of formation (the difference of sum of energies of individual atom and total energy of the Ti-doped compound) has been calculated and presented in Table 1. The negative value of enthalpy of formation ($^{\circ}H_f$) shows that all the compounds are thermodynamically stable in FM phase.

3.2 Elastic Properties

The elastic constants define the limits in which materials mechanical behavior can be identified. To calculate the elastic constants we use the *elast* package which solves non-linear differential equations for compatible solution and is implemented into WIEN2k code [28]. The application of symmetry operations on crystalline materials reduces the large number of elastic constants to three independent constants for cubic structure. Hence, three equations are required to find out these elastic constants. The first equation helps to calculate the elastic modulus associated to the bulk modulus (B_0), the second for volume conserving tetragonal strains, and the third for rhombohedral strain tensor that provides information about deformation [37]. The mechanical stability demands that $C_{11} - C_{12} > 0$, $C_{44} > 0$, $C_{11} + 2C_{12} > 0$, and $C_{12} < B_0 < C_{11}$ for a cubic lattice [38]. The predicted values of bulk modulus obtained from Murnaghan's equation of states of a cubic crystal as well as from elastic constants $B = (1/3)(C_{11} + 2C_{12})$ for $\text{Be}_{0.75}\text{Ti}_{0.25}\text{Y}$ (Y = S, Se, and Te) are almost equal. This confirms that the predicted results of elastic constants are reliable. The decreasing trend of elastic constants (C_{11} , C_{12} , and C_{44}) and bulk modulus with concentration Ti (see Table 2) shows that these materials are less stiff as mentioned earlier [39].

Fig. 4 Total density of states (TDOS) and partial density of states (PDOS) for $\text{Be}_{0.75}\text{Ti}_{0.25}\text{Se}$ alloy for majority spin (upwards arrow) and minority spin (downwards arrow) configuration using mBJLDA functional



The internal strain parameter or Kleinman parameter (ζ) describes the relative position of cation and anion in a crystal lattice and provides a measure of bond stretching (ζ approaching to zero) and bond bending (ζ approaching 1). ζ is calculated from the relation,

$$\xi = \frac{C_{11} + 8C_{12}}{7C_{11} + 2C_{12}} \quad (1)$$

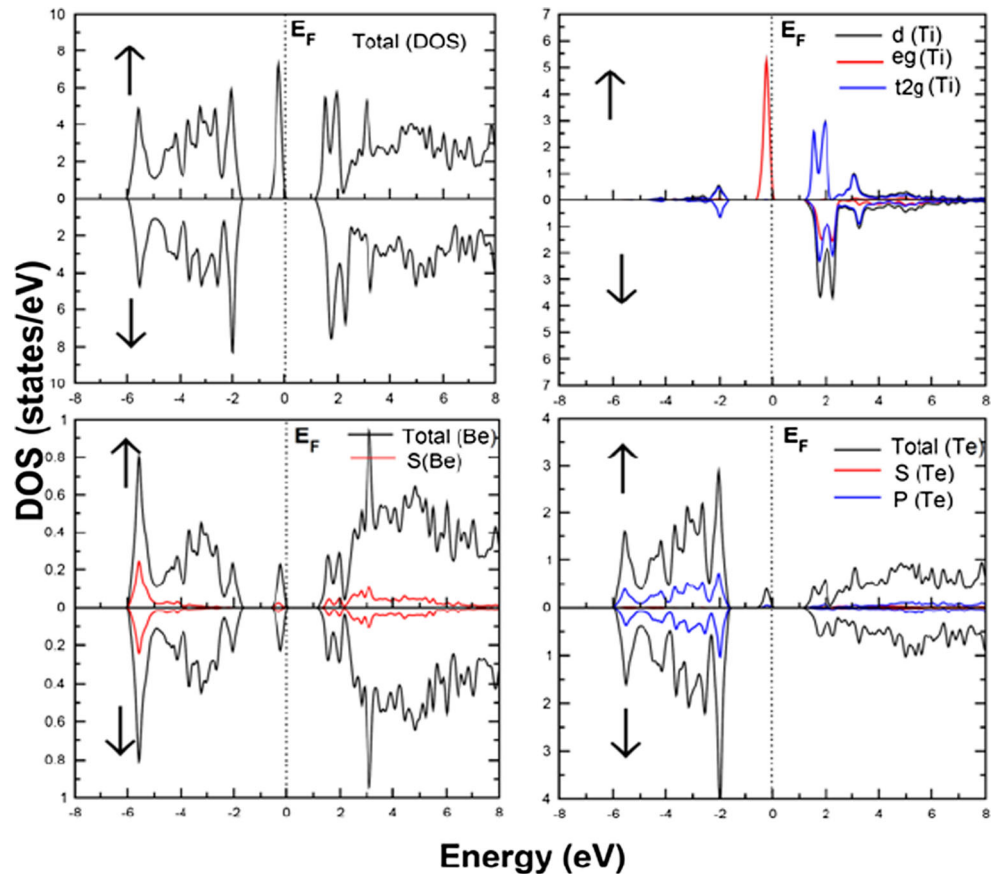
From our results, the value of Kleinman parameter shows a small increase that indicates that there is bond bending with the incorporation of Ti ions [40]. The elastic modulus, Young's modulus (E), shear modulus (G), and Poisson's ratio (ν) are also calculated from Voigt and Reuss–Hill approximation [41]. The relations $E = 9BG / (3B + G)$ and $\nu = (3B - 2G) / 2(3B + G)$ show the dependence of young modulus and Poisson's ratio on shear modulus and bulk modulus, respectively. The Poisson's ratio provides valuable information about the nature of force acting on crystalline materials. If the value of ν lies between 0.25 and 0.5, then forces among the atoms constituting the material are central. In our case, the value of Poisson's ratio does not lie between these two limits indicating that the nature of inter-atomic forces is non-central. Moreover, our calculated values of the Poisson's ratio also qualify the Ti-doped BeY compounds to be brittle since ν having a critical value below 0.26 is termed brittle. This can also be verified from the calculated in terms

of the Pough's ratio (B/G) which, by definition, has a value less than 1.75 for brittle materials.

3.3 Electronic Properties

The relaxed crystal structures obtained from the WC-GGA calculations are used to calculate the spin-polarized band structures for $\text{Be}_{0.75}\text{Ti}_{0.25}\text{Y}$ ($Y = \text{S}, \text{Se}, \text{and Te}$) in the first Brillouin zone along the high symmetry points. By using mBJLDA, the FM band structures for spin up state and spin down states for all the compounds under study are graphically presented in Fig. 2. From Fig. 2, it is clear that the majority spin channels saddle the Fermi level thus showing a metallic nature. On the other hand, the minority spin channel keeps semiconducting nature. As a result, the band structures of FM phase for Ti-doped BeY ($Y = \text{S}, \text{Se}, \text{and Te}$) show HM nature having an HM bandgap of 0.99, 1.19, and 1.21 eV for $\text{Be}_{0.75}\text{Ti}_{0.25}\text{S}$, $\text{Be}_{0.75}\text{Ti}_{0.25}\text{Se}$, and $\text{Be}_{0.75}\text{Ti}_{0.25}\text{Te}$, respectively. A clearer picture of HM nature of these compounds can be seen in the partial density of state (PDOS) plots shown in Figs. 3, 4, and 5. One can see that the 3d state of Ti splits into five degenerate states. In these five states, two states are termed e_g (d_{z^2} and $d_{x^2-y^2}$), while the remaining three states are termed t_{2g} (d_{xy} , d_{xz} , and d_{yz}) states. The movement of the t_{2g} state into conduction band with Ti doping creates a metallic effect in majority

Fig. 5 Total density of states (TDOS) and partial density of states (PDOS) for $\text{Be}_{0.75}\text{Ti}_{0.25}\text{Te}$ alloy for majority spin (upwards arrow) and minority spin (downwards arrow) configuration using mBJLDA functional



spin channel and justifies the compounds under study to be HMFs.

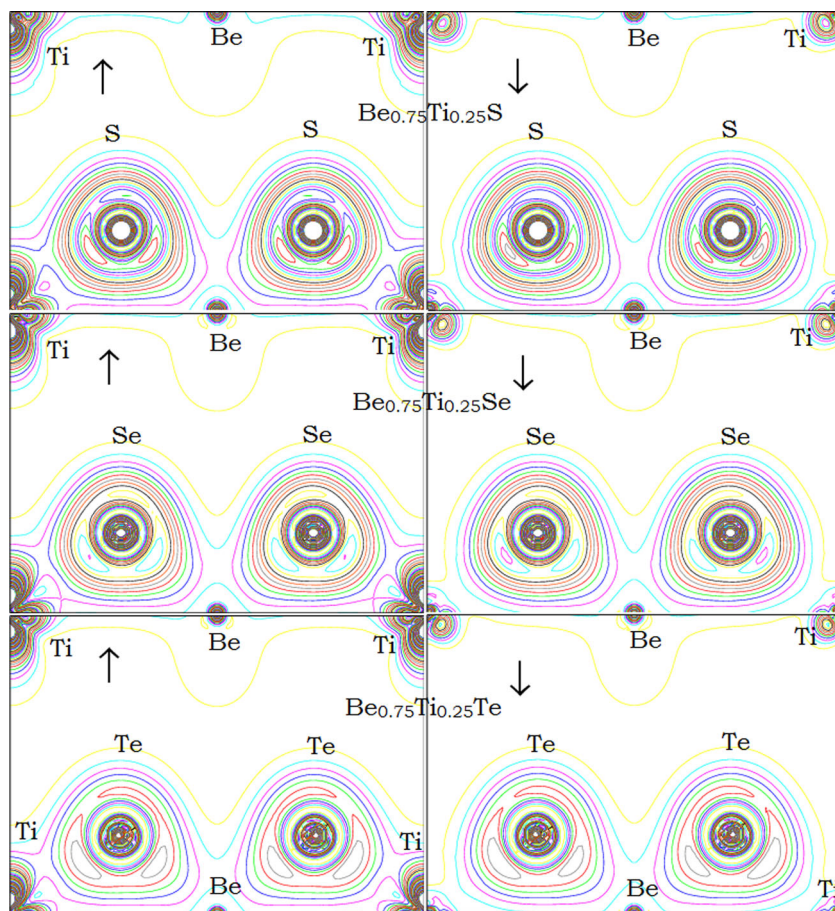
The calculated spin-polarized PDOS and total density of states (TDOS) for $\text{Be}_{1-x}\text{Ti}_x\text{Y}$ ($\text{Y} = \text{S}, \text{Se}, \text{and Te}$) at $x = 0.25$ are shown in Figs. 3, 4, and 5. According to the Alex Zunger criteria [42], it is clear that (in the energy range from -1 to 4 eV in spin up state and 1 to 4 eV in spin down state) the Ti- d state has strong interaction with S/Se/Te- p states around the Fermi level. Therefore, the pd coupling is strong near the periphery of Fermi level and becomes weak at other regions of energy for BeY ($\text{Y} = \text{S}, \text{Se}, \text{and Te}$). Moreover, the splitting of $3d$ state of Ti shifts towards lower energy in spin down channel and higher energy in spin up channel (because of unfilled d states of Ti) and creates some empty state in valence band that shows the introduction of p -type character into pure ferromagnetic semiconductor.

The pd hybridization creates a tetrahedral environment in which each atom has its four neighbors. In this tetrahedral geometry, fivefold degenerate transition metal $3d$ states split into threefold degenerate states (t_{2g}) and twofold degenerate states (e_g). The t_{2g} (antibonding state) is higher in energy than e_g (bonding state). Only the t_{2g} state is responsible for hybridization with p state of the host semiconductor to produce strong pd interaction, while the e_g state has zero contribution to the hybridization process. The crystal field energy was calculated using the relation $\Delta E_{\text{crystal}} = E_{t_{2g}} - E_{e_g}$. The exchange splitting $\Delta_x(pd)$ energies calculated from DOS plots are presented in Table 3. The negative values of exchange splitting energy show that the effective potential for minority spin is more attractive than majority spin, as is the case in spin-polarized systems. Another important parameter is the

Table 3 Crystal field energy ($\Delta E_{\text{crystal}}$), exchange splitting $\Delta_x(d)$, conduction band edge splitting (ΔE_C) and valance band edge splitting (ΔE_V), and exchange constants ($N_o\alpha$ and $N_o\beta$) calculated for all three $\text{Be}_{1-x}\text{Ti}_x\text{Y}$ ($\text{Y} = \text{S}, \text{Se}, \text{and Te}$) at $x = 0.25$ alloys

Compound	$\Delta E_{\text{crystal}}$	$\Delta_x(d)$	ΔE_C (eV)	ΔE_V (eV)	$N_o\alpha$	$N_o\beta$
$\text{Be}_{0.75}\text{Ti}_{0.25}\text{S}$	2.089	2.23	0.072	-3.24	0.388	-17.52
$\text{Be}_{0.75}\text{Ti}_{0.25}\text{Se}$	2.045	2.17	0.070	-2.50	0.377	-13.47
$\text{Be}_{0.75}\text{Ti}_{0.25}\text{Te}$	1.760	2.04	0.049	-1.64	0.251	-8.41

Fig. 6 Electron density plots of $\text{Be}_{0.75}\text{Ti}_{0.25}\text{Y}$ ($\text{Y} = \text{S}, \text{Se}, \text{Te}$) alloys majority spin (upwards arrow) and minority spin (downwards arrow) configurations using mBJLDA functional



spin exchange splitting energy $\Delta_x(d)$ of transition metal d state that is responsible for double exchange mechanism (the value of exchange splitting is greater than the crystal field energy that favors the ferromagnetism according to double exchange mechanism). The double exchange mechanism explains the ferromagnetic behavior of Ti-doped magnetic semiconductors. The values of exchange splitting $\Delta_x(d)$ and crystal field energy ($\Delta E_{\text{crystal}}$) are presented in Table 3.

In order to understand the charge transfer properties of spin-polarized $\text{Be}_{0.75}\text{Ti}_{0.25}\text{Y}$ compounds and elaborate on their bonding nature, we have computed the Be, Ti, and Y valence charge densities which are shown in Fig. 6. It is evident from the charge density contour plots that the

$\text{Be}_{0.75}\text{Ti}_{0.25}\text{Y}$ compounds have mixed ionic and covalent character for the Be–Y and Ti–Y bonds. The valence charge around the Be site is due to s orbitals, while the Y site shows both s and p valence charge states. The charge density appear to be similar at Be sites for the three compounds studied in this work with differences only appearing at the Y and Ti sites. The smaller electronegativity values of Te as compared to S results in the reduction of covalent bonding on going from $\text{Be}_{0.75}\text{Ti}_{0.25}\text{S}$ to $\text{Be}_{0.75}\text{Ti}_{0.25}\text{Te}$, which is also visible in the charge density contour plots (see Fig. 6).

Our calculations make it obvious that the ferromagnetism in $\text{Be}_{1-x}\text{Ti}_x\text{Y}$ ($\text{Y} = \text{S}, \text{Se}, \text{Te}$) alloys is mainly caused by the carrier-mediated mechanism. In the examined systems, the doped Ti atoms are the main source of holes

Table 4 Calculated magnetic moment at Be, Ti, and Y ($\text{Y} = \text{S}, \text{Se}, \text{Te}$) sites in $\text{Be}_{0.75}\text{Ti}_{0.25}\text{Y}$ alloys

Compound	Magnetic moments (in terms of Bohr magneton, μ_B)			
	Total	Be site	Ti site	Y site
$\text{Be}_{0.75}\text{Ti}_{0.25}\text{S}$	2.000	0.0238	1.479	−0.0031
$\text{Be}_{0.75}\text{Ti}_{0.25}\text{Se}$	2.000	0.0203	1.484	−0.0004
$\text{Be}_{0.75}\text{Ti}_{0.25}\text{Te}$	2.000	0.0204	1.561	−0.0005

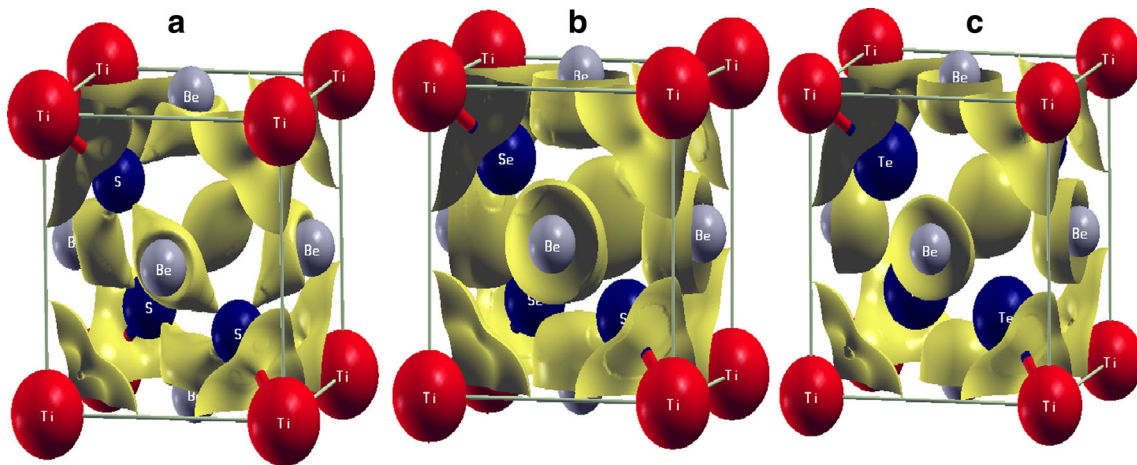


Fig. 7 Partial spin density plots for **a** $\text{Be}_{0.75}\text{Ti}_{0.25}\text{S}$, **b** $\text{Be}_{0.75}\text{Ti}_{0.25}\text{Se}$, and **c** $\text{Be}_{0.75}\text{Ti}_{0.25}\text{Te}$, where a yellow flower represents magnetic moment contribution of each atom

introduced due to the doping with Ti atom as shown in electronic band structures. The real origin of ferromagnetism is determined by the position of the impurity band. The double exchange interaction can describe the origin of ferromagnetism, if the impurity states situate in the band gap. The impurity bands of the minority spin channel are located in the band gap and the Fermi level falls within the impurity band of the minority spin channel, indicating significant numbers of holes and double exchange phenomenon causing ferromagnetism. Therefore, we conclude hole-mediated double exchange originates from the ferromagnetism in $\text{Be}_{1-x}\text{Ti}_x\text{Y}$ ($\text{Y} = \text{S}, \text{Se}, \text{and Te}$) alloys.

3.4 Magnetic Properties and Exchange Constants

The calculated values of total and local magnetic moments for $\text{Be}_{0.75}\text{Ti}_{0.25}\text{Y}$ ($\text{Y} = \text{S}, \text{Se}, \text{and Te}$) in muffin-tin region are shown in Table 4. The strong hybridization between crystal fields split level ($3t_{2g}$) of unfilled $3d$ state of Ti and p state of anion confirms the ferromagnetic behavior and reduces the local magnetic moment of Ti from its free space charge value. As a result, the reducing values of magnetic moments contribute to Be, S/Se/Te, and interstitial sites. Therefore, the pd exchange splitting of Ti-doped BeY ($\text{Y} = \text{S}, \text{Se}, \text{and Te}$) lowers the total energy of the system that confirms the stability of ferromagnetic state of the compounds. Further, in order to discuss the major part of magnetic moment that comes from Ti sites, we represent a spin-dependent density plot (overall effect of electron spin) in $1\ 1\ 0$ planes is given in Fig. 7a–c. From Fig. 7a–c, it is to be noted that the Ti sites in the three alloys are mostly localized with spin densities, and split $3d$ orbitals of Ti contribute mainly in the magnetic moment.

The $s - d$ exchange splitting ($N_0\alpha$) and $p - d$ exchange splitting ($N_0\beta$) that explains the ferromagnetism in diluted

magnetic semiconductors are calculated from the edge splitting of conduction band ($\Delta E_C = E_C^\downarrow - E_C^\uparrow$) and valence band ($\Delta E_V = E_V^\downarrow - E_V^\uparrow$) using the following equations [43]:

$$N_0\alpha = \frac{\Delta E_C}{x\langle S \rangle} \text{ and } N_0\beta = \frac{\Delta E_V}{x\langle S \rangle} \quad (2)$$

Here, x is the concentration of transition metal ion and $\langle S \rangle = \langle M \rangle / 2$ (where $\langle M \rangle$ is the total magnetic moment of all atoms in the unit cell). From Table 3, it can be seen that the lattice parameter has an inverse relation with exchange constants. Hence, the decreasing value of lattice parameter and negative value of $N_0\beta$ indicates that $p - d$ interaction is stronger than $s - d$ interaction that confirms the ferromagnetic nature of these materials. In addition, this opposite sign of $p - d$ interaction ($N_0\beta$) and $s - d$ interaction ($N_0\alpha$) represents the antiferromagnetic interaction, and a lower magnitude of $p - d$ interaction energy favors the ferromagnetism.

4 Conclusion

In our study, we have used spin-polarized DFT to investigate the structural, elastic, electronic, and magnetic properties of $\text{Be}_{0.75}\text{Ti}_{0.25}\text{Y}$ ($\text{Y} = \text{S}, \text{Se}, \text{and Te}$) compounds. The ferromagnetic semiconductor behavior of these materials is confirmed from band structure and density of state calculations. The calculated values of Pugh’s ratio and universal anisotropy factor show the ductile nature of the concerned compounds. The exchange splitting energies $\Delta_x(d)$ and $\Delta_x(pd)$ and exchange constants ($N_0\alpha$) and ($N_0\beta$) are elaborated from triple degeneracy t_{2g} state, and a negative value ($N_0\beta$) confirms that the nature of effective potential is more attractive in spin down case rather than that in spin up case. The opposite values of exchange constants ($N_0\alpha$) and ($N_0\beta$)

also show that the conduction and valence states behave in an antiferromagnetic way in exchange splitting process. The main part of total magnetic moment comes from the Ti site and the hybridization between the $3d$ state of Ti and the p state of S/Se/Te reduces the magnetic moment of Ti from its free space charge value and create traces of magnetic moment on non-magnetic Be and S/Se/Te sites.

Acknowledgments Asif Mahmood would like to extend his sincere appreciations to the Deanship of Scientific Research at King Saud University for funding this Prolific Research Group (PRG-1436-26). The author (M. Yaseen) is thankful to HEC Pakistan for funding this work (Grant No. 21-261/SRGP/R&D/HEC/2014).

References

- Arora, S., Manoharan, S.S.: *Opt. Mater.* **31**, 176 (2008)
- Karanjai, M.K., Gupta, D.D.: *Thin Solid Films* **155**, 309 (1987)
- Firszt, F., Wronkowska, A.A., Wronkowska, A., Legowski, S., Marasek, A., Meczynska, H., Pawlak, M., Paszkowicz, W., Strzalkowski, K., Zakrzewski, A.J.: *Cryst. Res. Technol.* **40**, 386 (2005)
- Furdyna, J.K.: *J. Appl. Phys.* **64**, R29 (1988)
- Wolf, S.A., Awschalom, D.D., Buhrman, R.A., Daughton, J.M., von Molnar, S., Roukes, M.L., Chtchelkanova, A.Y., Treger, D.M.: *Science* **294**, 1488 (2001)
- Twardowski, A., Swagten, H.J.M., Dejonge, W.J.M. In: Jain, M. (ed.) *Cobalt-based II-VI semimagnetic semiconductors*, pp. 227–254. World Scientific, Singapore (1993)
- Swagten, H.J.M., Twardowski, A., De Jonge, W.J.M., Demianiuk, M.: *Phys. Rev. B* **39**, 2568 (1989)
- Shand, P.M., Lewicki, A., Crooker, B.C., Giriat, W., Furdyna, J.K.: *J. Appl. Phys.* **67**, 5246 (1990)
- Alay-e-Abbas, S.M., Wong, K.M., Noor, N.A., Shaukat, A., Lei, Y.: *Solid State Sci.* **14**, 1525 (2012)
- Noor, N.A., Ali, S., Shaukat, A.: *J. Phys. Chem. Solids* **72**, 836 (2011)
- Sajjad, M., Zhang, H.X., Noor, N.A., Alay-e-Abbas, S.M., Younas, M., Abid, M., Shaukat, A.: *J. Supercond. Nov. Magn.* **27**, 2327 (2014)
- Dahmane, F., Tadjer, A., Doumi, B., Mesri, D., Aourag, H.: *Supercond. Nov. Magn.* **26**, 3339 (2013)
- Saeed, Y., Nazir, S., Reshak, A.H., Shaukat, A.: *J. Alloys Compd.* **508**, 245 (2010)
- Mahmood, Q., Javed, A., Murtaza, G., Alay-e-Abbas, S.M.: *Mater. Chem. Phys.* **162**, 831 (2015)
- Doumi, B., Tadjer, A., Dahmane, F., Djedid, A., Yakoubi, A., Barkat, Y.: *Supercond. Nov. Magn.* **27**, 1 (2013)
- Dietl, T.: *J. Appl. Phys.* **103**, 07D111 (2008)
- Kaspar, T.C., Droubay, T., Heald, S.M., Engelhard, M.H., Nachimuthu, P., Chambers, S.A.: *Phys. Rev.* **B77**, 201303R (2008)
- Wong, K.M., Alay-e-Abbas, S.M., Fang, Y., Shaukat, A., Lei, Y.: *J. Appl. Phys.* **114**, 034901 (2013)
- Wong, K.M., Alay-e-Abbas, S.M., Shaukat, A., Fang, Y., Lei, Y.: *J. Appl. Phys.* **113**, 014304 (2013)
- Furrer, A., Podlesnyak, A., Krämer, K.W., Embs, J.P., Pomjakushin, V., Strässle, T.H.: *Phys. Rev. B* **89**, 144402 (2014)
- Prinz, G.A.: *Science* **282**, 1660 (1998)
- Soulen, R.J., Byers, J.M., Osofsky, M.S., Nadgorny, B., Ambrose, T., Cheng, S.F., Broussard, P.R., Tanaka, C.T., Nowak, J., Moodera, J.S., Barry, A., Coey, J.M.D.: *Science* **282**, 85 (1998)
- de Groot, R.A., Mueller, F.M., van Engen, P.G., Buschow, K.H.J.: *Phys. Rev. Lett.* **50**, 2024 (1983)
- Kılıç, A., Kervan, N., Kervan, A.: *J. Supercond. Nov. Magn.* **28**, 1767 (2015)
- Arda, L., Acikgoz, M., Gungor, A.: *J. Supercond. Nov. Magn.* **25**, 2701 (2012)
- Boutaleb, M., Tadjer, A., Doumi, B., Djedid, A., Yakoubi, A., Dahmane, F., Abbar, B.: *J. Supercond. Nov. Magn.* **27**, 1603 (2014)
- Boutaleb, M., Doumi, B., Sayede, A., Tadjer, A., Mokaddem, A.: *J. Supercond. Nov. Magn.* **28**, 143 (2015)
- Błaha, P., Schwarz, K., Madsen, G.K.H., Kvasnicka, D., Luitz, J.: WIEN2k, An augmented plane wave plus local orbitals program for calculating crystal properties. Vienna University of Technology, Vienna (2001)
- Hohenberg, P., Kohn, W.: *Phys. Rev.* **136**, B864 (1964)
- Wu, Z., Cohen, R.E.: *Phys. Rev. B* **73**, 235116 (2006)
- Becke, A.D., Johnson, E.R.: *J. Chem. Phys.* **124**, 221101 (2006)
- Singh, D.J.: *Phys. Rev. B* **82**, 205102 (2010)
- Guo, S.D., Liu, B.G. *Euro Phys. Lett.* **93**, 47006 (2011)
- Muraghan, F.D.: *Proc. Natl. Acad. Sci. U.S.A.* **30**, 244 (1944)
- Eaith, M., Alhayek, I.: *Rev. Adv. Mater. Sci.* **21**, 183 (2009)
- Lam, P.K., Cohen, M.L., Martinez, G.: *Phys. Rev. B* **35**, 1991 (1987)
- Djedid, A., Doumi, B., Mecabih, S., Abbar, B.: *J. Mater. Sci.* **48**, 6074 (2013)
- Suna, Z., Li, S., Ahujab, R., Schneider, J.M.: *Solid State Commun.* **129**, 589 (2004)
- Schreiber, E., Anderson, O.L., Soga, N.: *Elastic Constants and Their Measurement*. McGraw-Hill, New York (1973)
- Kleinman, L.: *Phys. Rev.* **128**, 2614 (1962)
- Hill, R.: *Proc. Phys. Soc. London* **65**, 350 (1952)
- Huai, S., Zunger, A.: *Phys. Rev. B* **35**, 2340 (1987)
- Sanvito, S., Ordejon, P., Hill, N.A.: *Phys. Rev. B* **63**, 165206 (2001)
- Narayana, C., Nesamony, V.J., Ruoff, A.L.: *Phys. Rev. B* **56**, 14338 (1997)
- Luo, H., Chandehari, K., Green, R.G., Ruoff, A.L., Trailand, S.S., DiSalvo, F.J., et al.: *Phys. Rev. B* **52**, 7058 (1995)
- Okoye, C.M.I.: *Eur. Phys. J. B* **39**, 5 (2004)
- Yim, W.M., Dismakes, J.B., Stofko, E.J., Paff, R.J.: *J. Phys. Chem. Sol.* **33**, 501 (1972)
- Laref, S., Laref, A.: *Comp. Mat. Sci.* **51**, 135 (2012)
- Gonzalez-Diaz, M., Rodriguez-Hernandez, P., Munoz, A.: *Phys. Rev. B* **55**, 14043 (1997)